JOURNAL OF MATERIALS SCIENCE 31 (1996) 663–671

Isothermic growth of one spherulite around circular obstacles in a polypropylene foil

G. E. WERNER SCHULZE, M. BIERMANN
Abteilung für Werkstoffwissenschaft, Institut für Physik der Kondensierten Materie, Heinrich–Heine–Universität Düsseldorf, Universitätsstr. 1, Geb. 25.23, 40225 Düsseldorf, Germany

Growth of one spherulite within a thin foil of polypropylene around one circular obstacle or around combinations of circular obstacles is investigated. For each obstacle there exists a region of shadow, seen from the nucleus of the spherulite, which influences the growth of the spherulite. Within any region of shadow the growth fronts are evolvents of the obstacle's boundary, because the spherulite grows isotropically. When two growth fronts belonging to one spherulite meet each other inside the shadow, an intrinsic grain boundary is formed for each obstacle. Additionally, growth of one spherulite around a rectangular obstacle and a spherical obstacle is investigated.

1. Introduction

1.1. Spherulitic growth of isotactic polypropylene

An undercooled melt of polypropylene crystallizes by spherulitic growth. In this paper crystallization is studied in a foil of isotactic polypropylene (iPP) in the presence of obstacles. The used polymer possesses an isotacticity of 96%, a mean molecular weight, M_w, of 300000 and a thickness of 4 μm and contains neither stabilizers nor fillers. This foil melts at about 168 °C. This foil is put on a slide and temperature is increased at a heating rate of 10 °C min^{-1} to 200 °C in an N_2 inert atmosphere to avoid thermo-oxidation. The temperature then is reduced to 132 °C for isothermal crystallization. In the supercooled melt at 132 °C some nuclei of the α modified iPP are formed which start to grow circularly and simultaneously as α spherulites [1].

In the metastable molten foil at 132 °C the α-modification spherulite grows at a constant growth rate of $c_\alpha = 3.3\ \mu m\ min^{-1}$. The growth rate is reduced to about 0.3 μm min^{-1} at 144 °C. This effect is used for production of thermic marks or time marks at equidistant time intervals. Therefore, after crystallization at 132 °C for 15 min the temperature is increased as quickly as possible from 132 to 144 °C. This leads to a reduction of growth rate. After 4 min at 144 °C the temperature of the foil is again decreased to 132 °C for 15 min. This cycle is repeated as often as necessary. One obtains circular marks with different grey shading (Fig. 1), because the crystallinity of these marks is greater than that of the surrounding crystallized material. The marks show the run of the growth fronts at the chosen points of time [2].

Fig. 2 shows a schematic drawing of an undisturbed growing spherulite with the nucleus in its centre. The limiting circle between spherulite and undercooled melt is called the growth front. The two circular marks in the interior of the spherulite are called thermic marks or time marks. The radial rays from the nucleus to the growth front are called growth lines. The infinite number of growth lines is approximately described by the fibrils in the experiment. An exact description of the growth lines by the fibrils is not possible because of small-angle branching on the tip of the fibrils [3–5]. The growth lines always lie perpendicular to the growth fronts; they are orthogonal trajectories.

An isothermally crystallizing spherulite grows circularly because of the isotropy of spherulitic growth. Every point on the growth front of the spherulite is at the same distance, r, to the nucleus. r is only given by the growth rate, c, and the time of growth, t. In other words, all growth lines have the same and shortest length, r, at the same moment, t. Obviously, this describes a circle when spherulitic growth is undisturbed.

For a theoretical description one can treat the spherulites in the thin foil as nearly two-dimensional aggregates. This is so because foil with a thickness of 4 μm is thin compared to the mean spherulite diameter of 100 μm or more. So, one can use analytical two-dimensional geometry or differential planar curve geometry [6].

1.2. Spherulitic growth in the presence of obstacles

The situation of Fig. 1 is different in the presence of obstacles. These obstacles are static and unmovable. Fig. 3 shows the experimental result of the growth of one spherulite around one circular obstacle. The nucleus lies on the right side of the obstacle. One observes deformation of the growth fronts in a region of

0022–2461

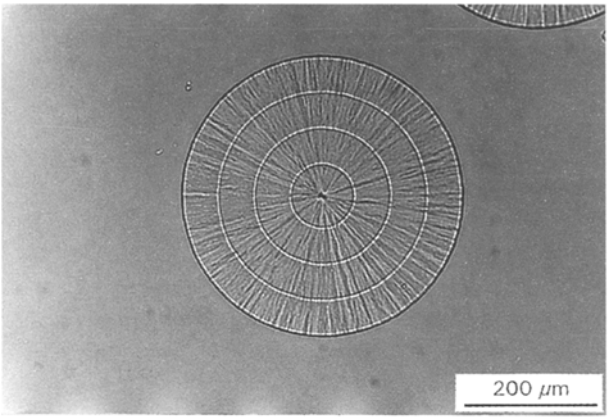

Figure 1 A circularly growing spherulite of α-modified isotactic polypropylene at 132 °C. In the interior of the spherulite three equidistant time marks set after every 15 min of isothermal crystallization can be found. The grain is completely surrounded by amorphous melt.

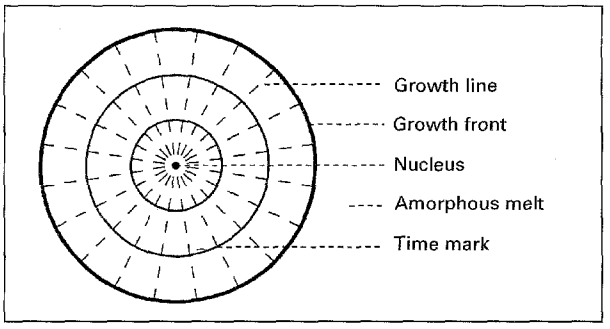

Figure 2 Schematic drawing of a circularly growing spherulite completely surrounded by amorphous melt with the nucleus in its centre. One realizes the run of the growth front, two thermic marks and a number of growth lines.

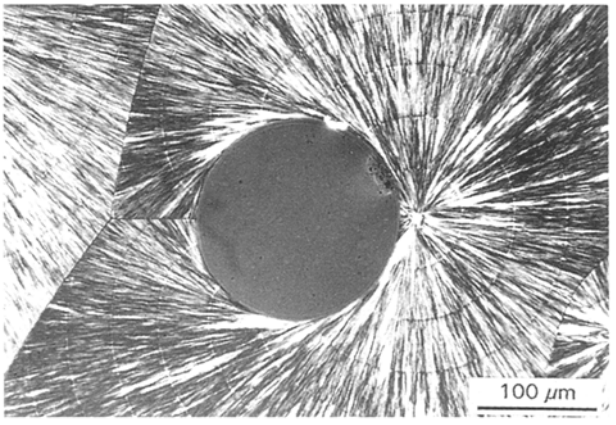

Figure 3 A spherulite growing around a circular obstacle. For photography, circularly polarized light was used and equidistant time marks were set. The diameter of the obstacle is 170 ± 3 μm. The nucleus is placed at the right side of the obstacle. On the left side, opposite to the nucleus, an intrinsic grain boundary can be seen.

shadow behind the obstacle and the appearance of an intrinsic grain boundary. The deformation of growth fronts can easily be seen by the run of time marks and fibrils.

During experimentation, such an obstacle is realized by producing a circular hole cut into the polypropylene foil. The foil is prepared according to the above given heat treatment. Then, a circular hole is made using a watchmaker's lathe, with which a pin of the desired diameter is made and suitably ground. Using this tool the hole is cut directly. After annealing some degrees below the melting point, the whole foil is covered at 20 °C with a suitable transparent glue in order to obtain a stable hole shape during the following heat treatment. The temperature is increased from 20 °C at 3 °C min^{-1} to 185 °C. This melt temperature is reduced by 10 °C min^{-1} to 132 °C, where some nuclei appear and start their growth. Sometimes the desired case is realized: one spherulite may lie near to the hole and has the possibility of growing around it, while all other spherulites that may form or that will appear at later points of time as "stragglers" may be sufficiently distant not to disturb this process.

For the case of one spherulite growing around an obstacle, the description of growth has to be modified partly. The growth lines are not allowed to pass through the interior of the obstacle, since there is no polymer melt. The consequence is that a growth shadow has to be taken into consideration. This growth shadow is defined by all areas that cannot be reached by a straight growth line outgoing from the nucleus, which is typical for undisturbed isothermal spherulitic growth.

The basic principle for description of the growth front inside the shadow region is the isotropy of spherulitic growth. Each point on the growth front at point of time, t, has *the same and shortest distance* to the nucleus.

Outside the shadow this principle leads to circular growth as mentioned above.

Inside the shadow the run of the growth front is exactly described by an imaginary, inextensible and stretched thread which unwinds the obstacle's boundary. The constructed curve is called evolvent in mathematics. The run of the thread itself defines the run of the growth lines inside the shadow. The unwound curve, in this case the circular obstacle, is called evolute in mathematics [7, 8]. One notes that the growth fronts are always perpendicular to the growth lines.

A second consequence of the existence of the obstacle is the necessary appearance of an intrinsic grain boundary [9, 10].

2. Discussion

2.1. One circular obstacle

2.1.1. Basic considerations

Now apply the concept of constructing an evolvent to the growth of one spherulite around one circular obstacle as shown in Fig. 3. Fig. 4 shows the growth shadow caused by one circular obstacle. The shadow is separated into an upper and a lower half because of the high symmetry of this case. The nucleus is positioned at A, a circular obstacle with radius R is centred at B. The distance between nucleus and centre of the circular obstacle is $d = \overline{AB}$. The growth rate of the spherulite equals c. This also is valid inside the shadow

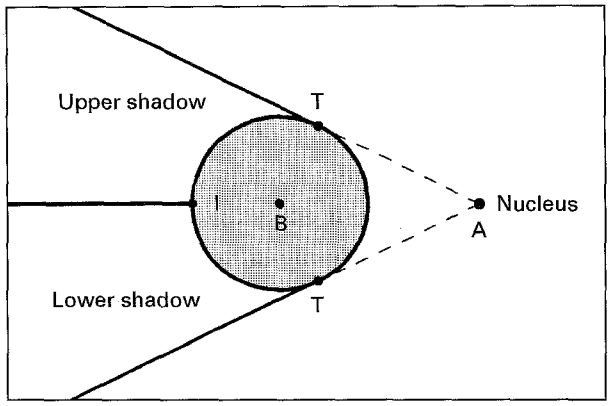

Figure 4 Schematic drawing of the growth shadow at a circular obstacle. Its centre is at B, and the nucleus lie at A. The upper and the lower part of the shadow both begin at T. Beginning at I, there runs an intrinsic grain boundary separating both parts of the shadow.

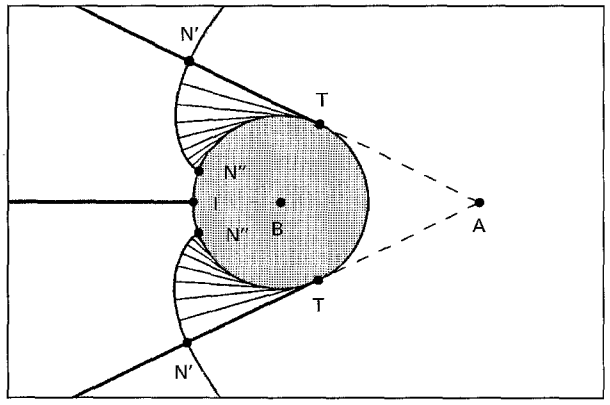

Figure 5 The run of one growth front belonging to a thread length, $l = \overline{TN}$ with a number of growth lines between their end points, N' and N'', in both parts of the shadow.

because of isotropy. The radius of growth then is $r = ct$ at time of growth, t.

Undisturbed and circular spherulitic growth ends at point of time

$$t_0 = \frac{d - R}{c} \tag{1}$$

The beginning of the growth shadow is marked by points T where the direction of growth of the spherulite is tangential to the obstacle's boundary. The shadow limits are tangents to the circle passing through the nucleus, A. It holds

$$t_T = \frac{(d^2 - R^2)^{1/2}}{c} \tag{2}$$

For $t_0 \leqslant t < t_T$ the growth fronts are circular arcs ending on the obstacle's boundary. For $t \geqslant t_T$ the growth fronts are evolvents of a circle inside the shadow which are continued by circular arcs around A outside the shadow. This is shown schematically in Fig. 5 [9].

2.1.2. Mathematical derivation of evolvent

For constructing the evolvent of the circular obstacle for points of time, $t_T \leqslant t < t_I$, one uses Fig. 6. The

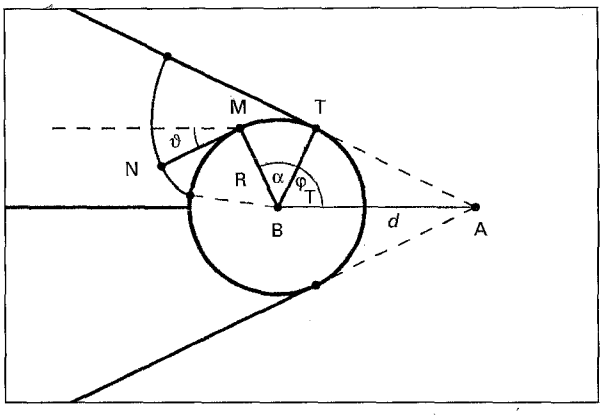

Figure 6 Construction of an evolvent of a circle inside the shadow region. A thread with length, $l = \overline{TN}$ is fixed at T and used for description of the run of the growth front.

centre of the co-ordinate system is positioned in the centre of the circle, B. This derivation is only demonstrated for the upper half because of symmetry. The tangential point, T, now possesses the co-ordinates

$$\begin{aligned} x_T &= R \cos \varphi_T \\ y_T &= R \sin \varphi_T \end{aligned} \tag{3}$$

with

$$\varphi_T = \cos^{-1} \frac{R}{d}$$

In T, one fixes the imaginary inextensible and stretched thread describing the run of the growth fronts inside the shadow. The thread has a length of

$$l(t) = \overline{TN} = c(t - t_T) \tag{4}$$

N is a point of this growth front. For construction one uses a parameter, α, describing the angle between points T and M of Fig. 6. The growth line runs along the circular arc between T and M and then, between M and N, in the direction of the tangent to the circle in M, up to point N belonging to the growth front. The total length of these two parts is l. Thus, l indicates one evolvent out of an infinite family of parallel curves, while any point on a special evolvent can be reached by variation of α. Total length, l, is an addition of these two lengths

$$l_1 = \overline{TM} = R\alpha$$

and

$$l_2 = \overline{MN} = l - l_1 = l - R\alpha$$

with

$$l = l_1 + l_2$$

The angle of the slope, ϑ, of a tangent to the circular arc in M amounts to

$$\vartheta = \varphi_T + \alpha - \frac{\pi}{2} \tag{5}$$

Thus, the co-ordinates of M are

$$\begin{aligned} x_M &= R \cos (\varphi_T + \alpha) \\ y_M &= R \sin (\varphi_T + \alpha) \end{aligned}$$

Point N is reached from M when following the tangent in M to the circle. It yields

$$x_N - x_M = -l_2 \cos \varphi$$
$$y_N - y_M = -l_2 \sin \varphi$$

According to this calculation one obtains as representative for all points on an evolvent of length, l, in cartesic co-ordinates by use of parameter α

$$x_N(l,\alpha) = R\cos(\varphi_T + \alpha) - (l - R\alpha)\sin(\varphi_T + \alpha)$$
$$y_N(l,\alpha) = R\sin(\varphi_T + \alpha) + (l - R\alpha)\cos(\varphi_T + \alpha) \quad (6)$$

The parameter α becomes a maximum when the complete length, l, is unwound on the circle's boundary, thus $l = R\alpha_m$. So, the permitted values for α are

$$0 \leqslant \alpha < \frac{l}{R} = \alpha_m \quad (7)$$

The growth lines are always perpendicular to the growth front, they are orthogonal trajectories of the growth front. Fig. 5 shows an example of the run of one growth front between their end points, N′ and N″, inside the shadow with a number of corresponding growth lines.

The length, s, of the growth front between N′ and N″ is obtained by integration over the element of arc which can be expressed by parametric representation $[x_N(\alpha), y_N(\alpha)]$. One obtains

$$s = \int_0^{\alpha_m} [\dot{x}_N^2(\alpha) + \dot{y}_N^2(\alpha)\, d\alpha^{1/2}]$$
$$= \int_0^{\alpha_m} (l - R\alpha)\, d\alpha$$
$$= \frac{1}{2} R\alpha_m^2 = \frac{1}{2}\frac{l^2}{R}$$

2.1.3. The intrinsic grain boundary

When growth reaches point I of Fig. 7, the formation of an intrinsic grain boundary begins. Here, two branches of the growth front, having grown around the obstacle in different directions, meet for symmetrical reasons. The intrinsic grain boundary must be a straight line. It yields for point I

$$\varphi_T + \alpha_I = \pi \text{ and } l_I = R\alpha_I.$$

The growth front reaches I at point of time

$$t_I = t_T + \frac{R}{c}(\pi - \varphi_T) \quad (8)$$

So, formation of the intrinsic grain boundary takes part for $t_I \leqslant t < \infty$. The lengths of the thread are $l \geqslant l_I$. For describing the formation of the intrinsic grain boundary one uses an angle, σ, between the two growth directions at the intrinsic grain boundary (Figs 7 and 8). The growth direction is given by the tangent to the circle passing through point J on the intrinsic grain boundary. The limiting cases for σ are $\sigma(t_I) = \pi$ and $\lim_{t\to\infty} \sigma(t) = 0$. According to Fig. 7, the

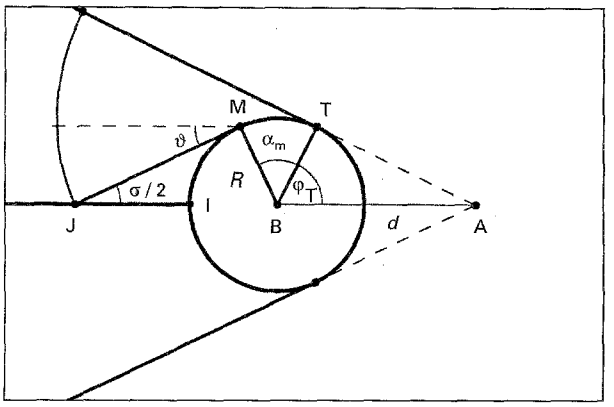

Figure 7 Schematic drawing for constructing the run of the intrinsic grain boundary using the angle σ. The length of the thread here is $l = \overline{TJ}$.

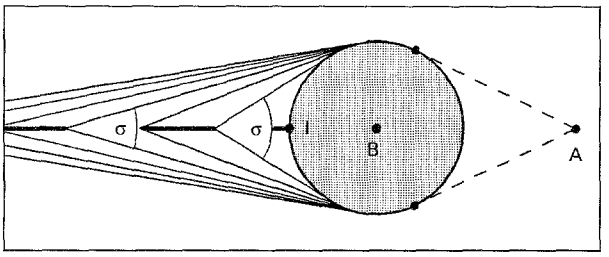

Figure 8 Reduction of the angle σ between the growth directions of the spherulite at the intrinsic grain boundary with increasing distance from the obstacle. The intrinsic grain boundary gets less and less pronounced.

angle $\sigma/2$ equals the slope of tangent, φ. The relation between the maximal angle, α_m, used for description of the run of the growth front and the angle σ is

$$\frac{\sigma(t)}{2} = \varphi_T + \alpha_m(t) - \pi/2$$

Since yields $\pi \geqslant \sigma(t) > 0$ depending on the position of J, one obtains $\pi - \varphi_T \geqslant \alpha_m > \pi/2 - \varphi_T$ as possible values for α_m. α has to be varied between 0 and α_m for description of the run of the growth front between the shadow limit and the intrinsic grain boundary.

Using $l_2 = \overline{MJ}$, one obtains the relation between $\sigma(t)$ and growth time, t

$$\cot\frac{\sigma(t)}{2} = \frac{l_2}{R}$$

Using $c(t_I - t_T) = R(\pi - \varphi_T)$, it yields

$$t = t_I + \frac{R}{c}\left[\cot\frac{\sigma(t)}{2} + \frac{\sigma(t)}{2} - \frac{\pi}{2}\right] \quad (9)$$

This relation is implicit and cannot be solved for σ. Fig. 8 shows the reduction of angle σ with increasing distance from the obstacle. The intrinsic grain boundary gets less and less pronounced.

The length $k(t) = \overline{IJ}$ of the intrinsic grain boundary is deduced from

$$\cos\frac{\sigma}{2} = \frac{l_2}{R + k}$$

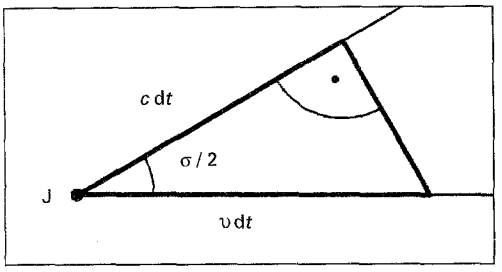

Figure 9 Calculation of the rate of formation, υ, of the intrinsic grain boundary out of the direction of growth of a spherulite with growth rate, *c*.

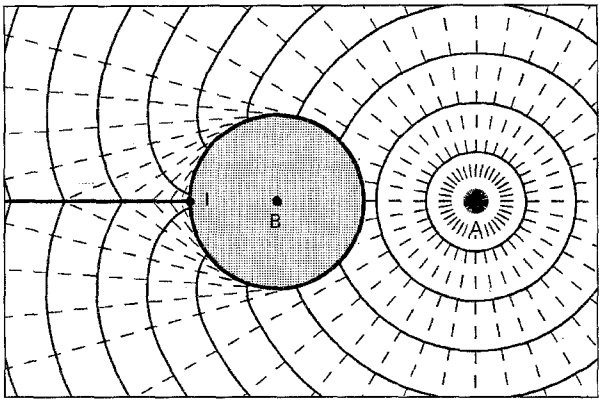

Figure 10 A complete description of one spherulite growing around a circular obstacle. Some growth lines, equidistant time marks and the intrinsic grain boundary are shown.

One obtains

$$k(\sigma) = R\left[\frac{1}{\sin(\sigma/2)} - 1\right] \qquad (10)$$

The rate of formation, v, of the intrinsic grain boundary is

$$v(t) = \frac{dk}{dt} = \frac{\partial k}{\partial \sigma}\frac{\partial \sigma}{\partial t} = \frac{\partial k}{\partial \sigma}\frac{1}{(\partial t/\partial \sigma)}$$

which gives

$$v(\sigma) = \frac{c}{\cos(\sigma/2)} \qquad (11)$$

with possible values $\infty \geqslant v(\sigma) > c$. This result can also easily be seen using Fig. 9. Expressed by the length of the intrinsic grain boundary, one obtains

$$v(k) = \frac{c}{\cos[\sigma(k)/2]} = \frac{c(k + R)}{(k^2 + 2kR)^{1/2}}$$

Fig. 10 shows the complete growth of one spherulite around one circular obstacle summarizing all presented considerations. The identity between theoretical description and experiment of Fig. 3 is convincing.

2.2. Two circular obstacles

Now investigate how one spherulite grows around combinations of two circular obstacles of the same and of different size. Since each growth around one obstacle causes the appearance of one intrinsic grain boundary, one will expect the appearance of two intrinsic grain boundaries at growth around two obstacles.

2.2.1. Two circles with the same radii

Fig. 11 shows an example of one spherulite growing around a combination of two circular obstacles of the same size with characteristic formation of two intrinsic grain boundaries as the experimental result.

Fig. 12 shows a schematic drawing of this situation. Regard two points, one and two, which are the centres of two circles with radius, *R*. The two centres have a distance of 3*R*. The nucleus in point A is exactly arranged on an arc of a circle around point one with a radius of 2*R*. α is the angle between the straight line that connects the two centres of the circles, one and two, and the straight line that connects the centre of circle one and the nucleus in A. Possible values for α are between α = 0 and 138.59° because of symmetry as Fig. 12 shows.

Both intrinsic grain boundaries are straight lines beginning on the boundary of the corresponding obstacle. These two intrinsic grain boundaries can possess different directions of growth which causes an

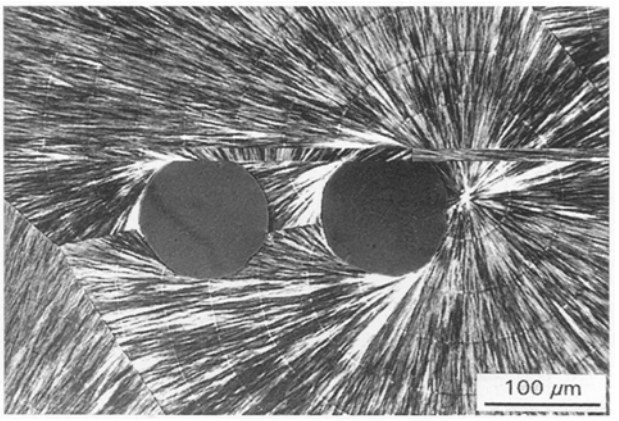

Figure 11 One spherulite is growing around two circular obstacles of the same size with a diameter of 110 ± 3 µm. Circularly polarized light was used for photography. The nucleus of the spherulite is placed at the right side of this combination of obstacles. The equidistant time marks and two intrinsic grain boundaries with the same slope can be recognized.

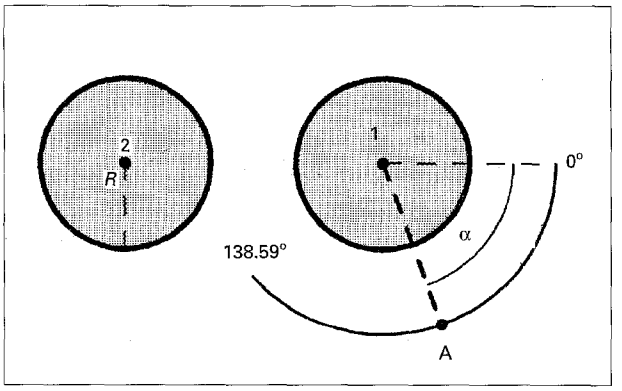

Figure 12 Two circular obstacles with radius, *R*, and centres at points one and two, respectively, have a distance of 3*R*. The nucleus at *A* lies at a distance of 2*R* to the centre of circle one. The angle α is shown.

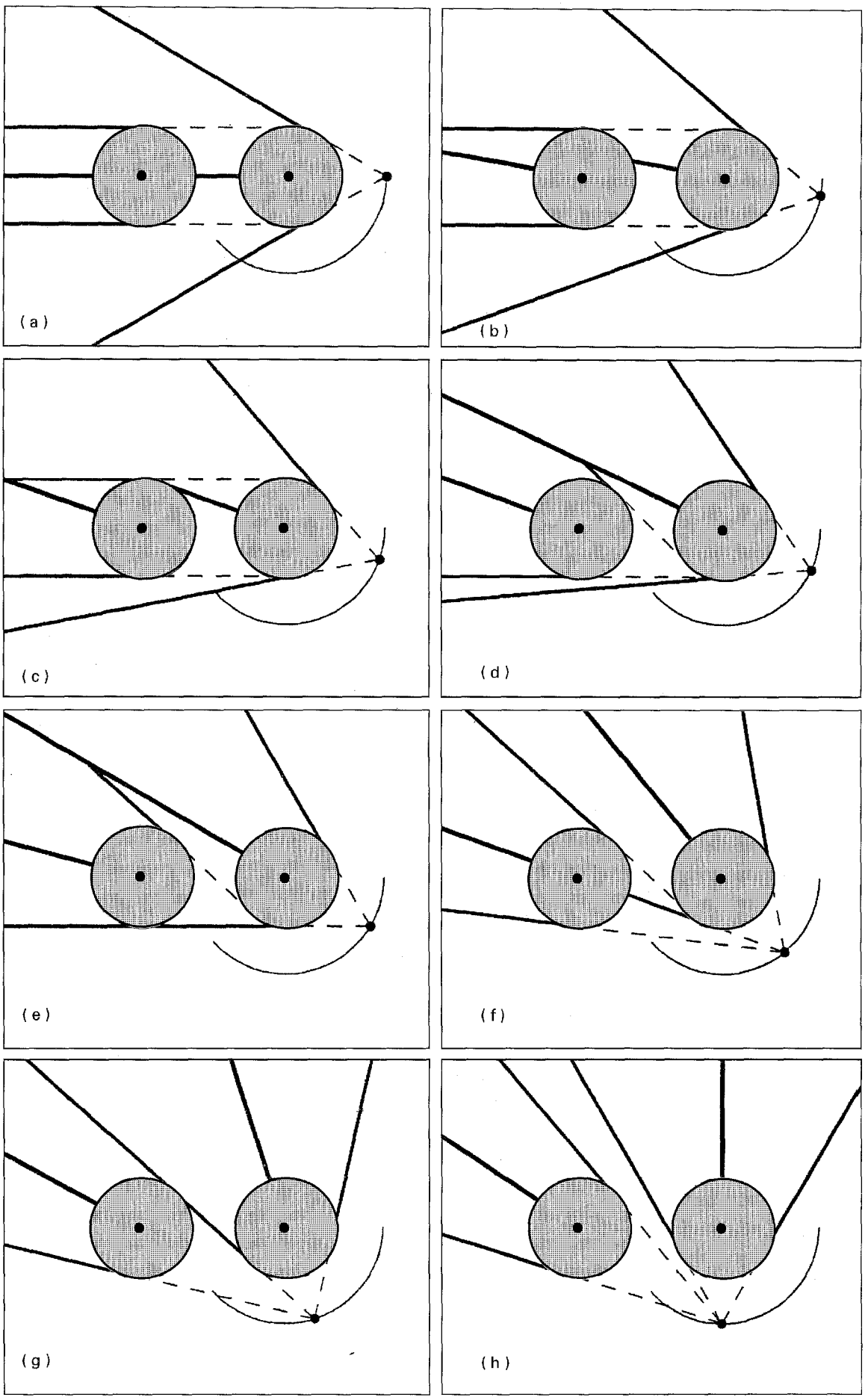

Figure 13 Eight basic possibilities of combining two circular obstacles of the same size when one single spherulite is growing around them. The position of the nucleus is marked by a point. Each of the combinations (a–h) possesses a characteristic run of the limitations of the shadow regions at both obstacles and of the two appearing intrinsic grain boundaries.

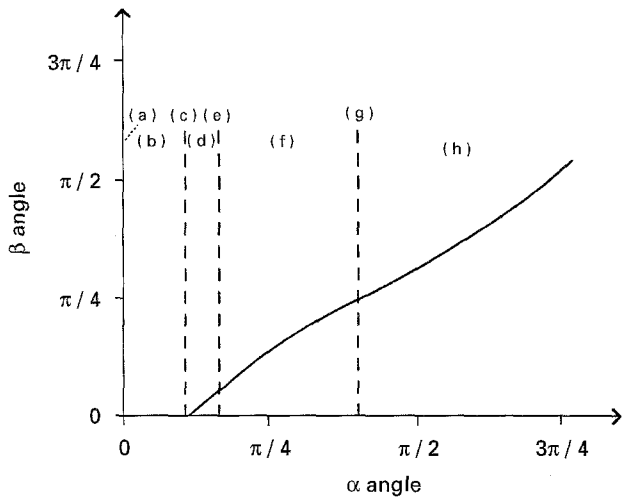

Figure 14 The difference in direction between the two intrinsic grain boundaries, β, as a function of α. For better comparison, the letters (a–h) mark the values or regions of values for α of the corresponding drawings of Fig. 13.

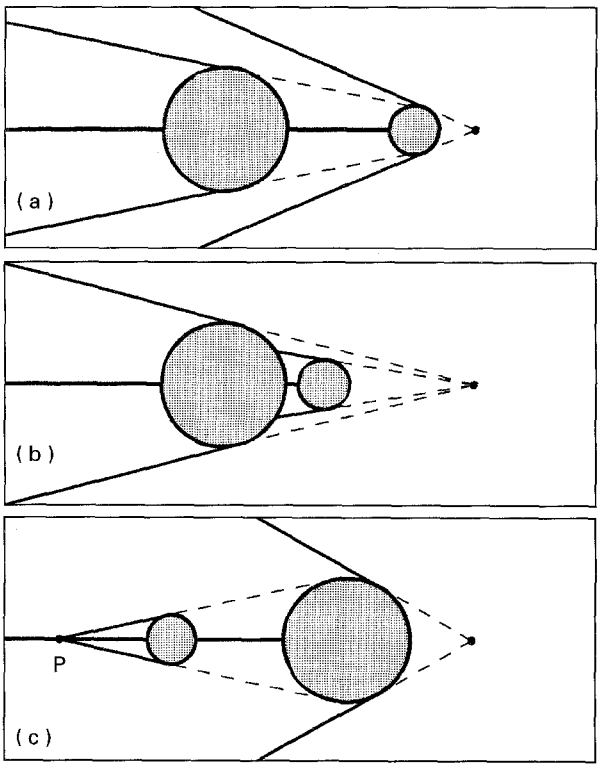

Figure 15 Three basic possibilities of growth shadow formation at two circular obstacles of different size. The nucleus, marked by the point on the right side, and the centres of the two obstacles lie on one straight line. The limitations of the regions of shadow and the intrinsic grain boundaries are drawn.

angle β between these directions. The correlation between the angles α and β is graphically shown in Fig. 13a–h. This figure shows eight basic possibilities of arranging the two circular obstacles and the nucleus. Additionally, they show the run of the intrinsic grain boundaries and of the limitations of the shadow regions.

Fig. 14 shows the angle β as a function of angle α as a result of computer calculation. The eight cases of Fig. 13 are marked by the corresponding letters.

With increasing distance from the obstacle a very small deviation from the straight line is possible if the intrinsic grain boundary intersects a limitation of the shadow region. This deviation has been neglected.

2.2.2. Two circles with different radii

Here one only investigates the completely symmetric case, with the nucleus and two centres of the obstacles lying on one straight line. The possible combinations contain all basic considerations for extending the presented concept to asymmetric cases as shown in Fig. 13.

One has to divide the concept into three basic cases, as shown in Fig. 15a–c. In each case the intrinsic grain boundary that is formed by evolvents of the first obstacle begins its growth on the boundary of the first obstacle and ends on the boundary of the second obstacle. This is not true for case (c) where the first intrinsic grain boundary consists of two parts, namely a first part between the two obstacles and a second part from P to infinity.

In each case the second intrinsic grain boundary begins its growth on the boundary of the second obstacle and ends in infinity. This is not true for case (c) where the second intrinsic grain boundary ends at point P. Of course, P cannot be seen in the experiment.

2.3. Growth around more than two circular obstacles

Since the growth of one spherulite around one obstacle causes the appearance of one intrinsic grain boundary, one obtains for two, three, four, . . . , circular obstacles the number of two, three, four, . . . , intrinsic grain boundaries, respectively.

Fig. 16 shows an arrangement of four circular obstacles of the same size. One spherulite is growing around these obstacles. The nucleus is placed at the lower right side of the obstacles. There are four straight intrinsic grain boundaries, each beginning at one of the circular obstacles. This picture demonstrates how to build up more complex

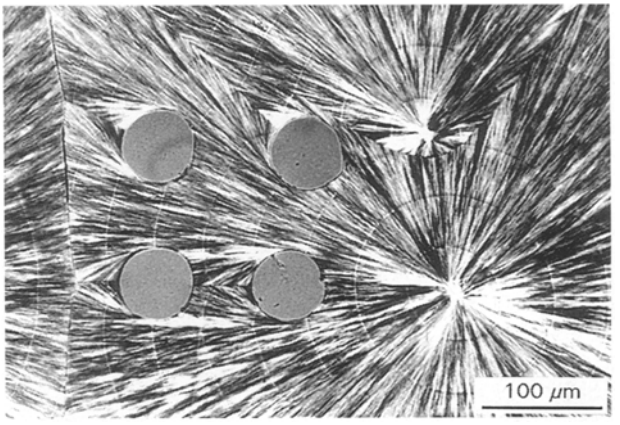

Figure 16 One spherulite is growing around an arrangement of four circular obstacles with a diameter of 60 ± 3 μm each. The nucleus is lying in the lower right corner. A second grain growing at the top cannot disturb the process of overgrowing. Circularly polarized light was used for photography. Equidistant time marks and four straight intrinsic grain boundaries can be seen.

structures out of a few basic units like, in this case, growth around one or two circular obstacles.

3. Conclusions

It has been demonstrated that in the presence of obstacles a growth shadow must be taken into consideration when investigating spherulitic crystallization processes. Within the shadow region, the growth fronts can be described as evolvents of the obstacle. An intrinsic grain boundary will appear after each growth around an obstacle. The basic concept for these considerations is the isotropic spherulitic growth.

Although circular obstacles were used for demonstration, the given considerations are independent of the special shape of the obstacle.

A similar concept is used for description of the formation of a common grain boundary between two growing spherulites with different growth rates [6, 11].

Appendix

A1. A rectangular obstacle

The presented concept can easily be extended to arbitrary shapes of the obstacle. Use the example of a rectangular obstacle [10]. Fig. A1 shows the experimental result, with typical deformation of growth fronts inside the shadow region and the appearance of one intrinsic grain boundary.

Fig. A2 shows a schematic drawing for describing the growth of one spherulite around a rectangular obstacle with the nucleus placed at point A. In this case, one has to separate different shadow regions which all originate in one of the four corners K, L, M, N, of the rectangle. The limits of the regions of shadow are named *k*, *l*, *m*, *n*.

The construction of evolvents leads to growth fronts which are always arcs of a circle, but with different centres of curvature. Outside the shadow, the centre of curvature of the growth fronts is the position of the nucleus, A. Inside each region of shadow, however, the centre of curvature of the growth fronts inside this part of the shadow is the corresponding corner of the rectangular obstacle. Whenever the growth front reaches a corner, a new region of shadow is entered. This fact is underlined by drawing a set of growth fronts with different line types in each shadow region of Fig. A2.

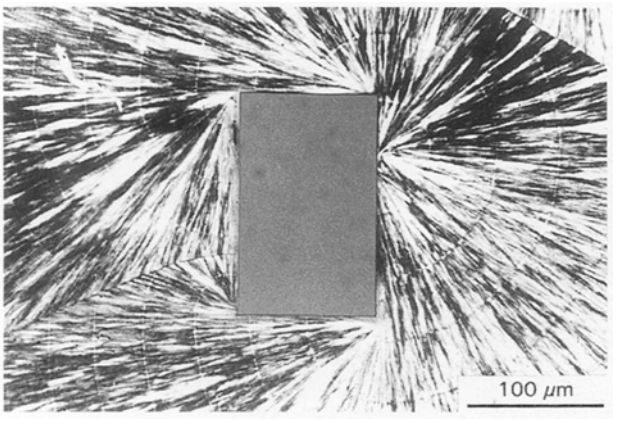

Figure A1 One spherulite growing around a rectangular obstacle. Circularly polarized light was used for photography. The obstacle has a length of 100 ± 3 μm and a height of 160 ± 3 μm. The nucleus is placed exactly on the right edge of this obstacle. At every 15 min of crystallization at 132 °C a thermic mark was set.

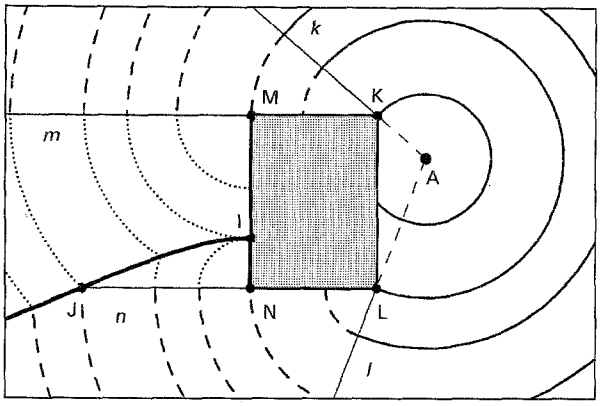

Figure A2 Schematic description of one spherulite growing around a rectangular obstacle. The nucleus is placed at *A*. At each corner of the obstacle, K, L, M, N, one limit of a region of shadow, *k*, *l*, *m*, *n*, originates. Inside each shadow region the growth fronts are circular arcs with centres of curvatures in the corresponding corners. This fact is underlined by different line types of the shown growth fronts at characteristic points of time. At I, the growth of an intrinsic grain boundary as hyperbola begins. At J, when the intrinsic grain boundary intersects the limit of shadow, *n*, a second and different branch of a hyperbola with the same tangent at J is formed.

Beginning in I, an intrinsic grain boundary is formed. It has the shape of a hyperbola, which can easily be obtained from its geometric definition. Each point on the hyperbola possesses a constant difference of distance to the foci N and M. Beginning in J, a hyperbola with foci L and M, but with the same tangent at J, can be observed when the intrinsic grain boundary intersects the limit, *n*, between two regions of shadow.

A2. Growth around a spherical inclusion

To apply the two-dimensional considerations presented in this paper to the three-dimensional case of growth around a spherical inclusion instead of a circular obstacle, one uses rotational symmetry according to the axis $\overline{AB}$. It is easy to imagine the shape of growth fronts. The spherulite grows spherically in the regions outside the (now three-dimensional) shadow. Inside the shadow the growth fronts are deformed because of growth around the spherical inclusion. The growth fronts are always perpendicular to the border of the inclusion. The one-dimensional intrinsic grain boundary in the two-dimensional region of shadow now becomes a one-dimensional channel in the three-dimensional shadow region. This one-dimensional channel appears because the intrinsic grain boundary is part of the rotational axis.

Therefore each spherulite that is growing undisturbed by other spherulites around a spherical inclusion possesses a channel directly. The channel damages some properties of the polymer, e.g. bond strength, corrosion rate and breakdown voltage.

Acknowledgements

This work is part of the dissertation of Dr M. Biermann, Heinrich–Heine–Universität Düsseldorf (1994) [6]. We are indebted to the Deutsche Forschungsgemeinschaft, DFG, for financial support.

References

1. J. VARGA, *J. Mater. Sci.* **27** (1992) 2557.
2. G. E. W. SCHULZE and H.-P. WILBERT, *J. Mater. Sci. Lett.* **8** (1989) 71.
3. H. D. KEITH and F. J. PADDEN, *J. Appl. Phys.* **35** (1964) 1270.
4. *Idem, ibid.* **35** (1964) 1286.
5. F. J. PADDEN and H. D. KEITH, *ibid.* **44** (1973) 1217.
6. M. BIERMANN, PhD thesis, Heinrich–Heine–Universität Düsseldorf, (1994).
7. I. N. BRONSTEIN and K. A. SEMENDJAJEW, "Taschenbuch der Mathematik" (Verlag Harri Deutsch, Thun und Frankfurt am Main, 1984) pp. 594–95.
8. M. M. LIPSCHUTZ, "Theory and Problems of Differential Geometry" (McGraw Hill, New York, 1969) pp. 80–102.
9. G. E. W. SCHULZE and M. BIERMANN, *J. Mater. Sci. Lett.* **12** (1993) 11.
10. *Idem, ibid.* **12** (1993) 533.
11. G. E. W. SCHULZE and H.-P. WILBERT, *Colloid & Polym. Sci.* **267** (1989) 108.

Received 23 September 1994
and accepted 8 June 1995